Progress In Electromagnetics Research M, Vol. 95, 1–12, 2020

Slotted Spherical Antenna with a Multi-Element Diaphragm in the Waveguide

Sergey L. Berdnik, Victor A. Katrich, Victor I. Kijko, Mikhail V. Nesterenko*, and Yuriy M. Penkin

Abstract—A problem of electromagnetic wave radiation by narrow slots cut in an end wall of a semi-infinite waveguide section into space above a perfectly conducting sphere is solved in a strict self-consistent formulation by the generalized method of induced magnetomotive forces (MMF). Inside the waveguide section, a reentrant cavity formed by the volume between a slotted diaphragm and the waveguide end wall is located. The waveguide is operating in the frequency range of a single-mode regime. The electrodynamic characteristics of this radiating system with the spherical screen of resonant dimensions are investigated numerically and experimentally. The possibility to develop the spherical antennas with a narrow-band frequency, energy, and spatial characteristics is substantiated.

1. INTRODUCTION

In all sectors of the economy and other spheres of modern society life, microelectronic robotics, information technologies, and radio communications are being applied at an increasing rate. Most of the devices used in these spheres are functioning in close proximity to each other both in the physical space and in frequency ranges. Therefore, a practically important problem concerning electromagnetic compatibility (EMC) of electronic systems exposed to interference from other electronic devices and natural phenomena arises. If the levels of the intrasystem and intersystem EMC do not reach the required values for all permissible variations of the equipment parameters, additional technical measures, for example, appropriate frequency filters in the transceiver paths should be used. In particular, such filters for slot antennas with waveguide excitation that do not impair their mass and size characteristics can be realized by waveguide resonant diaphragms [1].

As known in [2], non-protruding slotted radiators are widely used on mobile objects, since slot antennas do not significantly change their aerodynamic properties. The application of such antennas ranges from spacecrafts [3] to autonomous microprobes [4]. Quite often, a body of a mobile objects or their structural part can be approximately modelled by spherical surfaces, whose radii are comparable with the antenna operating wavelength. For example, spherical antennas are used for microwave hyperthermia allowing deep controlled heating of various tissues and organs of a living organism [5]. Therefore, interest in slotted spherical antennas with resonant spheres dimensions radiating into complex media has not disappeared for several decades.

The characteristics of spherical antennas with resonant rectangular slot radiator were studied in [6–12]. The external electrodynamic characteristics of slot antennas were considered in [6–8] under the assumption that the magnetic currents along the narrow half-wave slot radiator are defined by using a predefined cosine distribution. In the monograph [13], the authors of this article have proposed a numerical-analytical method known as the generalized method of induced MMF for solving the

Received 8 May 2020, Accepted 7 July 2020, Scheduled 29 July 2020

* Corresponding author: Mikhail V. Nesterenko (Mikhail.V.Nesterenko@gmail.com).

The authors are with the Department of Radiophysics, Biomedical Electronics and Computer Systems, V. N. Karazin Kharkiv National University, 4, Svobody Sq., Kharkiv 61022, Ukraine.

diffraction problems concerning slotted coupling elements between electrodynamic volumes. This method was applied for solving the problem of electromagnetic wave radiations by waveguide-slot structures into the external space above a perfectly conducting sphere [9–12]. The problem of electromagnetic wave radiation into space outside the perfectly conducting sphere through the slot cut in the end wall of the semi-infinite rectangular waveguide, known as the waveguide-slot spherical antenna (WSSA), was presented in a strict electrodynamic formulation in [9]. It was shown that the spherical screen shape with corresponding design parameters does not significantly limit the operating frequency band obtained for the waveguide-slot radiator placed over the infinite flat screen.

As known, a combination of internal resonators and slot radiators with pronounced frequency-selective properties allows us to obtained for such antennas required narrow-band frequency-energy and spatial characteristics [14–16]. Note that the results in [14, 15] were obtained for the slot excitation by a voltage generator. This article is aimed at investigation of electrodynamic characteristics of the WSSA [9] with the reentrant resonator formed by the one or two slot resonant diaphragm and waveguide end wall. Since simulation of multielement waveguide structures by using existing commercial programs are low-efficient, the boundary-value problem is proposed to solve in a rigorous, self-consistent formulation by the generalized method of induced MMF.

2. THE PROBLEM FORMULATION AND SOLUTION

Geometry of the WSSA and adopted notations are shown in Fig. 1. Let us consider three electrodynamic volumes separated by perfectly conducting wall: a semi-infinite rectangular waveguide, rectangular resonator, and space over a sphere marked by the indices Wg, R, and Sp, respectively, coupling with each other through rectilinear slots S_1, S_2, S_3 cut in common walls. The waveguide cross-section is $\{a \times b\}$, the resonator dimensions are $\{a \times b \times H\}$ and the sphere radius is R. A fundamental H_{10}-wave propagates in the waveguide from the region $z = \infty$. Let us introduce a Cartesian coordinate system associated with the waveguide and a spherical coordinate system associated with the sphere (Fig. 1). Cartesian coordinates of geometric centers of the internal slot aperture are $(a/2, y_{03}, 0)$, and the spherical coordinates of the external slot aperture are $(R, \pi/2, 0)$. The length of the external slot aperture along the sphere is $2L_3^e$. The diaphragm thickness of the with the slots S_1 and S_2 is equal to h. The slot center coordinates are $(a/2, y_{0m}, H)$. The slot S_3 radiates into space with material parameters ε_1, μ_1.

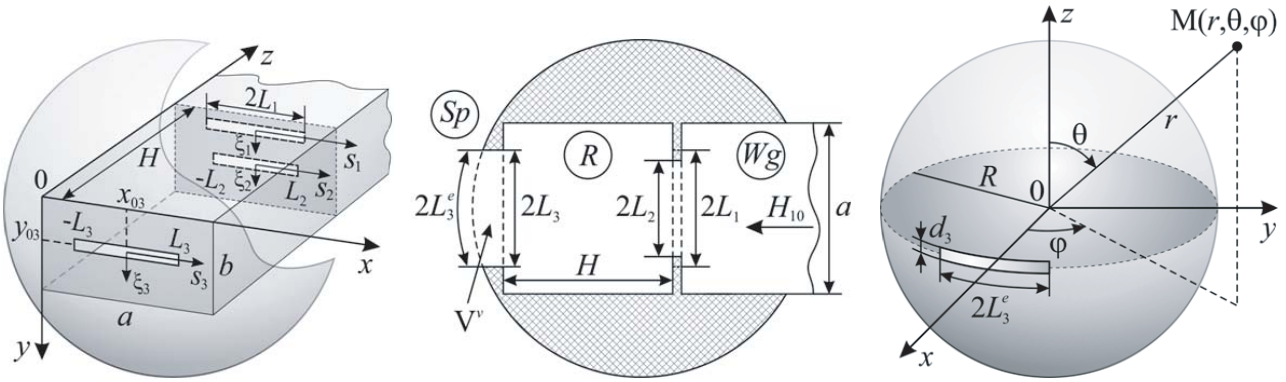

Figure 1. Geometry of the WSSA and corresponding notations.

The slot dimensions satisfy the following inequalities

$$\frac{d_m}{2L_m} \ll 1, \quad \frac{d_m}{\lambda} \ll 1, \quad m = 1, 2, 3, \tag{1}$$

where $2L_m$ and d_m are the length and width of the slots, and λ is the wavelength in free space. The

equivalent magnetic currents in the slots can be represented in the form

$$\vec{J}_m(s_m) = \vec{e}_{s_m} J_{0m} f_m(s_m) \chi_m(\xi_m), \tag{2}$$

where $\vec{e}_{s_m}$ are unit vectors; s_m and ξ_m are local coordinates associated with the slots; J_{0m} is the current amplitude, and the axes $\{0\xi_m\}$ are located in the plane $x = a/2$. The functions $f_m(s_m)$ must satisfy the boundary conditions $f_m(\pm L_m) = 0$. The functions $\chi_m(\xi_m)$ take into account the electric field behavior on the edges of the slots [13, 17] and satisfy the normalization conditions $\int\limits_{\xi_m} \chi_m(\xi_m) d\xi_m = 1$. For the infinitely thin diaphragm $h = 0$, these functions can be presented as

$$\chi_m(\xi_m) = \frac{1/\pi}{\sqrt{(d_m/2)^2 - \xi_m^2}}. \tag{3}$$

If the diaphragm thickness is finite ($h \neq 0$), and the slot edges are perfectly conducting rectangular wedges, the function $\chi_m(\xi_m)$ can be written as

$$\chi_m(\xi_m) = \frac{\Gamma(7/6)/\Gamma(2/3)}{\sqrt{\pi}(d_m/2)\sqrt[3]{1 - (2\xi_m/d_m)^2}}, \tag{4}$$

where $\Gamma(x)$ is the gamma function.

The functions $f_{1,2}(s_{1,2})$ and $\{f_3^e(\varphi)\ (f_3(s_3))\}$ were obtained as approximate solutions of the integral equation for the magnetic currents in the resonant slots cut in the diaphragm in the waveguide excited by the H_{10}-wave. The functions defining magnetic currents in the slot cut in the perfectly conducting sphere excited by a plane electromagnetic wave, whose vector $\vec{H}$ is parallel to the vector $\vec{e}_{s_3}$ [13], can be written as

$$\begin{gathered} f_{1,2}(s_{1,2}) = \cos k s_{1,2} \cos\frac{\pi L_{1,2}}{a} - \cos k L_{1,2} \cos\frac{\pi s_{1,2}}{a}, \\ f_3^e(\varphi) = \cos(k_1 R\varphi)\cos(\pi L_3^e/a) - \cos k_1 L_3^e \cos(\pi R\varphi/a), \quad f_3(s_3) = \cos k s_3 - \cos k L_3. \end{gathered} \tag{5}$$

Using continuity conditions for the tangential components of the magnetic field on the slot surfaces and the generalized method of induced MMF for the multi-slot structure, we obtain a system of algebraic equations relative to the unknown current amplitudes J_{0m}

$$\begin{cases} J_{01}\left(Y_{11}^{Wg} + Y_{11}^{R}\right) + J_{02}\left(Y_{12}^{Wg} + Y_{12}^{R}\right) + J_{03} Y_{13}^{R} = -\dfrac{i\omega}{2k} \displaystyle\int\limits_{-L_1}^{L_1} f_1(s_1) H_{0s_1}(s_1)\, ds_1, \\ J_{02}\left(Y_{22}^{Wg} + Y_{22}^{R}\right) + J_{01}\left(Y_{21}^{Wg} + Y_{21}^{R}\right) + J_{03} Y_{23}^{R} = -\dfrac{i\omega}{2k} \displaystyle\int\limits_{-L_2}^{L_2} f_2(s_2) H_{0s_2}(s_2)\, ds_2, \\ J_{03}\left(Y_{33}^{R} + Y_{33}^{Sp}\right) + J_{01} Y_{31}^{R} + J_{02} Y_{32}^{R} = 0, \end{cases} \tag{6}$$

where

$$Y_{mm}^{Wg,R,(Sp)} = \frac{1}{2k(k_1)} \int\limits_{-L_m}^{L_m} f_m(s_m) \left[\left(\frac{d^2}{ds_m^2} + k^2(k_1^2)\right) \int\limits_{-L_m}^{L_m} f_m(s'_m) G_{s_m}^{Wg,R,Sp}(s_m, s'_m) ds'_m\right] ds_m \tag{7}$$

are intrinsic slot conductivities and

$$Y_{mn}^{Wg,R} = \frac{1}{2k} \int\limits_{-L_{m,n}}^{L_{m,n}} f_{m,n}(s_{m,n}) \left[\left(\frac{d^2}{ds_{m,n}^2} + k^2\right) \int\limits_{-L_{n,m}}^{L_{n,m}} f_{n,m}(s'_{n,m}) G_{s_{m,n}}^{Wg,R}(s_{m,n}, s'_{n,m}) ds'_{n,m}\right] ds_{m,n} \tag{8}$$

are mutual slot conductivities; $G_s^{Wg,R,Sp}$ are s-components of quasi-one-dimensional ($|\xi_m - \xi'_m| \approx d_m/4$) Green's functions for the vector potentials of the corresponding volumes (see Appendix A); $H_{0s_{1,2}}(s_{1,2})$ are projections of fields of external sources on the axis of the slots, $k = 2\pi/\lambda$, and $k_1 = k\sqrt{\varepsilon_1 \mu_1}$.

The magnetic Green's functions of a semi-infinite rectangular waveguide, rectangular resonator, and space outside the perfectly conducting sphere (see Appendix A) allow us to derive, based on Eqs. (5), (7), (8), the expressions for the intrinsic and mutual slot conductivities

$$
\begin{aligned}
Y^{Wg}_{mn}(kL_m,kL_n) =& \frac{4\pi}{ab}\sum_{m=1,3\ldots}^{\infty}\sum_{n=0}^{\infty}\frac{\varepsilon_n\left(k^2-k_x^2\right)}{kk_z}\cos k_y y_{0m}\cos k_y\left(y_{0n}+\frac{d_{en}}{4}\right)I_1(kL_m)I_1(kL_n),\\
Y^{R}_{mn}(kL_m,kL_n) =& \frac{4\pi}{ab}\sum_{m=1,3\ldots}^{\infty}\sum_{n=0}^{\infty}\frac{\varepsilon_n\left(k^2-k_x^2\right)}{kk_z}\coth k_z H\\
&\times\cos k_y y_{0m}\cos k_y\left(y_{0n}+\frac{d_{en}}{4}\right)I_1(kL_m)I_1(kL_n),\\
Y^{R}_{m3}(kL_m,kL_3) =& Y^{R}_{3m}(kL_3,kL_m)=\frac{4\pi}{ab}\sum_{m=1,3\ldots}^{\infty}\sum_{n=0}^{\infty}\frac{\varepsilon_n}{k_z sh k_z H}\\
&\times\cos k_y y_{0m}\cos k_y\left(y_{03}+\frac{d_{e3}}{4}\right)I_1(kL_m)I_2(kL_3),\\
Y^{R}_{33}(kL_3) =& \frac{4\pi}{ab}\sum_{m=1,3\ldots}^{\infty}\sum_{n=0}^{\infty}\frac{\varepsilon_n k}{k_z\left(k^2-k_x^2\right)}\coth k_z H\cos k_y y_{03}\cos k_y\left(y_{03}+\frac{d_{e3}}{4}\right)I_2^2(kL_3),\\
Y^{Sp}_{33}(k_1L^e_3,k_1R) =& -\frac{4}{k_1R\mu_1}\sum_{n=1}^{\infty}\frac{1}{n(n+1)}\cdot\frac{1}{(n+1)-k_1Rh^{(2)}_{n+1}(k_1R)/h^{(2)}_n(k_1R)}\\
&\times\left\{(k_1R)^2C_0^2A^0_n\tilde{A}^0_n-2\sum_{m=1}^{n}C_m^2\left[m^2\left(n(n+1)-(k_1R)^2\right)B^m_n\tilde{B}^m_n-(k_1R)^2A^m_n\tilde{A}^m_n\right]\right\},
\end{aligned}
\tag{9}
$$

where

$$
\begin{aligned}
I_1(kL_m) &= 2\left\{\frac{k\sin kL_m\cos k_xL_m-k_x\cos kL_m\sin k_xL_m}{k^2-k_x^2}\cos\frac{\pi L_m}{a}\right.\\
&\left.-\frac{\left(\frac{\pi}{a}\right)\sin\frac{\pi L_m}{a}\cos k_xL_m-k_x\cos\frac{\pi L_m}{a}\sin k_xL_m}{(\pi/a)^2-k_x^2}\cos kL_m\right\},\\
I_2(kL_3) &= 2\frac{k_x\sin kL_3\cos k_xL_3-k\cos kL_3\sin k_xL_3}{k_x},\\
A^m_n &= \sqrt{\frac{\pi}{C_{nm}}}\Phi^m_n,\quad \tilde{A}^m_n=\sin\theta\frac{d\bar{P}^m_n(\cos\theta)}{d\theta}\bigg|_{\theta=\frac{\pi}{2}+\frac{d_e}{4R}},\\
B^m_n &= \sqrt{\frac{\pi}{C_{nm}}}F^m_n,\quad \tilde{B}^m_n=\bar{P}^m_n\left(\cos\left(\frac{\pi}{2}+\frac{d_e}{4R}\right)\right),\\
C_m &= \frac{\cos(\pi L^e_3/a)}{m^2-(k_1R)^2}\left[m\sin\frac{mL^e_3}{R}\cos k_1L^e_3-k_1R\cos\frac{mL^e_3}{R}\sin k_1L^e_3\right]\\
&-\frac{\cos k_1L^e_3}{m^2-(\pi R/a)^2}\left[m\sin\frac{mL^e_3}{R}\cos\frac{\pi L^e_3}{a}-\frac{\pi R}{a}\cos\frac{mL^e_3}{R}\sin\frac{\pi L^e_3}{a}\right]=C^I_m-C^{II}_m,\\
C^I_m\big|_{m\to k_1R} &= \left(\frac{L^e_3}{2R}+\frac{\sin(2k_1L^e_3)}{4k_1R}\right)\cos\frac{\pi L^e_3}{a},\quad C^{II}_m\big|_{m\to\frac{\pi R}{a}}=\left(\frac{L^e_3}{2R}+\frac{\sin(2\pi L^e_3/a)}{4\pi R/a}\right)\cos k_1L^e_3,
\end{aligned}
$$

$\bar{P}^m_n(\cos\theta)=\sqrt{\pi/C_{nm}}P^m_n(\cos\theta)$ are the normalized associated Legendre functions, $k_x=\frac{m\pi}{a},k_y=\frac{n\pi}{b},k_z=\sqrt{k_x^2+k_y^2-k^2}$, m and n are integers, $\varepsilon_n=\begin{cases}1, n=0\\ 2, n\neq 0\end{cases}$, and y_{0m} are coordinates of the slot centers.

The slot currents can be found by solving the equations system in Eq. (6). If the H_{10}-wave with the amplitude H_0 propagates in the semi-infinite rectangular waveguide, the fields can be presented as $H_{0s_{1,2}}(s_{1,2}) = 2H_0 \cos\frac{\pi s_{1,2}}{a}$. Then the field reflection coefficient S_{11} and the power radiation coefficient $|S_\Sigma|^2$ can be written as

$$S_{11} = \left\{1 - \frac{8\pi k_g}{iabk^3}\left[\tilde{J}_{01}F(kL_1) + \tilde{J}_{02}F(kL_2)\right]\right\} e^{-i2k_g z}, \tag{10}$$

$$|S_\Sigma|^2 = 1 - |S_{11}|^2, \tag{11}$$

where $\tilde{J}_{0m} = J_{0m}(-\frac{i\omega}{k^2}H_0)^{-1}$ arethe normalized currents amplitude in the slots, and $k_g = \sqrt{k^2 - (\pi/a)^2}$ is the propagation constant, and

$$F(kL_m) = 2\cos\frac{\pi L_m}{a}\frac{\sin kL_m \cos\frac{\pi L_m}{a} - \frac{\pi}{ka}\cos kL_m \sin\frac{\pi L_m}{a}}{1-(\pi/ka)^2} - \cos kL_m \frac{\sin\frac{2\pi L_m}{a} + \frac{2\pi L_m}{a}}{(2\pi/ka)}.$$

The equivalent width d_{e3} of the slot was calculated by the formula $d_{e3} \approx d_3 \exp(-\frac{\pi h_e}{2d_3})$ under the condition $(h_3 d_3/\lambda^2) \ll 1$, where $h_e = V^v/S_3$, V^v is the volume of the slot cavity, S_i the internal slot aperture area, and h_3 the maximum dimension of the slot tunnel cavity in the radial direction [9]. The thickness of the diaphragm wall was taken into account using a similar formula under condition $h_e = h$.

3. RADIATION FIELDS OF THE WSSA

The formula for determining the magnetic current on the slot aperture in space outside the sphere according to Eqs. (5) and (9) is

$$J(s) = -\frac{i\omega}{k_1^2}H_0 F(kL_3)\frac{[\cos(k_1 s)\cos(\pi L_3^e/a) - \cos k_1 L_3^e \cos(\pi s/a)]}{Y_{33}^R(kL_3) + Y_{33}^{Sp}(k_1 L_3^e, k_1 R)}. \tag{12}$$

The distribution of the slot magnetic current in Eq. (12) allows us to calculate the electrodynamic characteristics of the spherical antenna in a space outside the sphere. The total radiation field of the spherical antenna (Fig. 1(c)) can be determined by two components of the electric Hertz vector, $\Pi_{e\theta}^m(r,\theta,\varphi)$ and $\Pi_{e\varphi}^m(r,\theta,\varphi)$ [9], after substituting the current distribution $J(s) = J(R\varphi')$ in Eq. (12). Then the components of the total radiation field of the spherical antenna can be presented as:

$$\begin{aligned}
E_{er}(r,\theta,\varphi) &= -\frac{1}{r}\sum_{n=0}^{\infty} Q_n(r)\left(\begin{array}{l}\frac{FC_0(\varphi)}{2C_{n0}}P_n(\cos\theta)\left.\frac{dP_n(\cos\theta')}{d\theta'}\right|_{\theta'=\pi/2} \\ +\sum_{m=1}^{\infty}\frac{FC_m(\varphi)}{C_{nm}}P_n^m(\cos\theta)\,\Phi_n^m\end{array}\right), \\
E_{e\theta}(r,\theta,\varphi) &= \frac{1}{r}\sum_{n=0}^{\infty}\sum_{m=0}^{n}\frac{\varepsilon_m Q_n^*(r)\,FC_m(\varphi)}{2n(n+1)C_{nm}}\left[m^2\frac{P_n^m(\cos\theta)}{\sin\theta}F_n^m + \frac{dP_n^m(\cos\theta)}{d\theta}\Phi_n^m\right], \\
E_{e\varphi}(r,\theta,\varphi) &= -\frac{1}{r}\sum_{n=0}^{\infty}\sum_{m=1}^{n}\frac{mQ_n^*(r)\,FS_m(\varphi)}{n(n+1)C_{nm}}\left[\frac{dP_n^m(\cos\theta)}{d\theta}F_n^m + \frac{P_n^m(\cos\theta)}{\sin\theta}\Phi_n^m\right], \\
H_{er}(r,\theta,\varphi) &= -\frac{1}{i\omega\mu_1 r^2}\sum_{n=0}^{\infty}\sum_{m=1}^{n}\frac{mFS_m(\varphi)}{C_{nm}}\left(Q_n^*(r) - 2Q_n(r)\right)P_n^m(\cos\theta)\,F_n^m, \\
H_{e\theta}(r,\theta,\varphi) &= \frac{k_1^2}{i\omega\mu_1}\sum_{n=0}^{\infty}\sum_{m=1}^{n}\frac{Q_n(r)m\,FS_m(\varphi)}{n(n+1)C_{nm}}\left[\begin{array}{l}\frac{P_n^m(\cos\theta)}{\sin\theta}\Phi_n^m \\ +\left(1-\frac{n(n+1)}{(k_1 r)^2}\right)\frac{dP_n^m(\cos\theta)}{d\theta}F_n^m\end{array}\right], \\
H_{e\varphi}(r,\theta,\varphi) &= \frac{k_1^2}{i\omega\mu_1}\sum_{n=0}^{\infty}\sum_{m=0}^{n}\frac{Q_n(r)\,FC_m(\varphi)}{2n(n+1)C_{nm}}\left[\begin{array}{l}\varepsilon_m\frac{dP_n^m(\cos\theta)}{d\theta}\Phi_n^m \\ +2m^2\left(1-\frac{n(n+1)}{r^2}\right)\frac{P_n^m(\cos\theta)}{\sin\theta}F_n^m\end{array}\right],
\end{aligned} \tag{13}$$

where

$$Q_n(r) = \frac{h_n^{(2)}(k_1 r)}{(n+1)h_n^{(2)}(k_1 R) - k_1 R\, h_{n+1}^{(2)}(k_1 R)}, \quad F_n^m = P_n^m(\cos\theta')\big|_{\theta'=\pi/2}, \quad \Phi_n^m = \left.\frac{dP_n^m(\cos\theta')}{d\theta'}\right|_{\theta'=\pi/2}$$

$$FC_m(\varphi) = \int\limits_{-L_e/R}^{L_e/R} f(\varphi')\cos\left(m(\varphi-\varphi')\right)d\varphi', \quad FS_m(\varphi) = \int\limits_{-L_e/R}^{L_e/R} f(\varphi')\sin\left(m(\varphi-\varphi')\right)d\varphi',$$

$$C_{nm} = \frac{2\pi\,(n+m)!}{(2n+1)\,(n-m)!}, \quad Q_n^*(r) = \frac{\partial}{\partial r}\left(rQ_n(r)\right) = \frac{(n+1)h_n^{(2)}(k_1 r) - k_1 r\, h_{n+1}^{(2)}(k_1 r)}{(n+1)h_n^{(2)}(k_1 R) - k_1 R\, h_{n+1}^{(2)}(k_1 R)},$$

$$\varepsilon_m = \begin{cases} 1, & m = 0, \\ 2, & m \neq 0, \end{cases}$$

m and n are integers, and $h_n^{(2)}(k_1 r)$ and $h_{n+1}^{(2)}(k_1 r)$ are the spherical Hankel functions of the second kind.

Formulas (13) allow us to find electromagnetic fields at any distance from the antenna under condition $r \geq R$. If the external homogeneous medium is lossless, and ε_1, μ_1 are purely real quantities, Equations (13) in the antenna far zone ($r \gg \lambda$) are simplified, since the terms proportional to $1/r^2$ and $1/r^3$ can be omitted. As an example, we present here only the explicit expressions for components of the magnetic field of the WSSA.

$$\begin{aligned} H_{er}(r,\theta,\varphi) &= 0, \\ H_{e\theta}(r,\theta,\varphi) &= \frac{k_1^2}{i\omega\mu_1}\sum_{n=0}^{\infty}\sum_{m=1}^{n}\frac{Q_n(r) m\, FS_m(\varphi)}{n(n+1)C_{nm}}\left[\frac{P_n^m(\cos\theta)}{\sin\theta}\Phi_n^m + \frac{dP_n^m(\cos\theta)}{d\theta}F_n^m\right], \\ H_{e\varphi}(r,\theta,\varphi) &= \frac{k_1^2}{i\omega\mu_1}\sum_{n=0}^{\infty}\sum_{m=0}^{n}\frac{Q_n(r)\, FC_m(\varphi)}{2n(n+1)C_{nm}}\left[\varepsilon_m\frac{dP_n^m(\cos\theta)}{d\theta}\Phi_n^m + 2m^2\frac{P_n^m(\cos\theta)}{\sin\theta}F_n^m\right]. \end{aligned} \tag{14}$$

Since the relations $k_1 r \to \infty$ and $|k_1 r| \gg n$ are satisfied in the antenna far zone, the spherical Hankel functions of the second kind can be replaced by asymptotic representation $h_n^{(2)}(kr) \approx (i)^{n+1}\frac{e^{-ikr}}{kr}$, and the functions $Q_n(r)$ in Eq. (14) can be written as

$$Q_n(r) \approx \frac{e^{-k_1 r}}{k_1 r}\cdot\frac{(i)^{n+1}}{(n+1)h_n^{(2)}(k_1 R) - k_1 R\, h_{n+1}^{(2)}(k_1 R)}.$$

4. NUMERICAL AND EXPERIMENTAL RESULTS

Figure 2 shows the curves of the power radiation coefficient, $|S_\Sigma|^2$, as functions of the wavelength in the single-mode range of the rectangular waveguide with cross section $\{23 \times 10\}\,\mathrm{mm}^2$ for three variants of the WSSA. The curves corresponding to the various numbers of slots marked as: curve 1 — slot S_3, curve 2 — slots S_1 and S_3, 3 — slots S_1, S_2, and S_3. The WSSA parameters are as follows: $R = 80/\pi$ mm. $2L_1 = 2L_3 = 16$ mm, $2L_2 = 14$ mm, $d_1 = d_2 = d_3 = 0.8$ mm, $y_{01} = b/8$, $y_{02} = b/2$, $y_{03} = b/2$, $h = 1.0$ mm, $H = a/2$.

The plots show that the reentrant cavity placed in the waveguide substantially increases the system Q-factor. The resonance curve has a large steepness, and its shape approaches to a rectangular form (Fig. 2, Fig. 3). The second slot in the diaphragm gives rise to the total reflection of the incident H_{10}-wave ($|S_{11}| = 1.0$, $|S_\Sigma|^2 = 0$) at some wavelength depending upon the slot length $2L_2$ and position. In this case, the passband at half power level is substantially reduced in comparison with the cases of single- and double-slot structures. The radiation coefficient increases at shorter wavelengths, and its maximum position, λ_{res}/λ_c, depends on the geometric dimensions and position of the slot on the diaphragm. The maximum position can be found by the formula [13]

$$\frac{\lambda_{res}}{\lambda_c} = \frac{2L_2/a}{1 + \alpha(2/\pi)F\,(a, b, L_2, d_{e2}, y_{02})}, \tag{15}$$

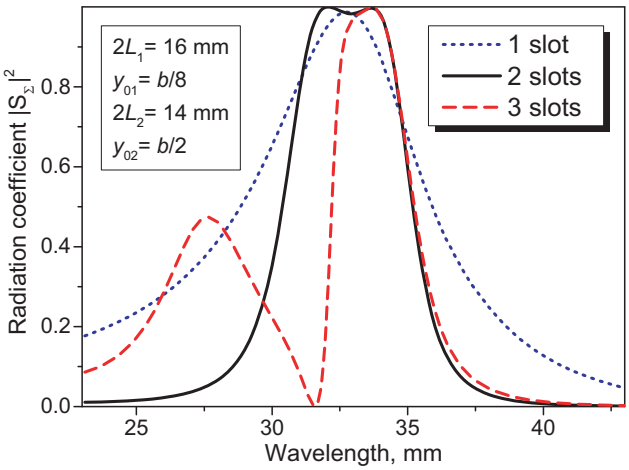

Figure 2. The power radiation coefficient $|S_\Sigma|^2$ of the WSSA versus the wavelength.

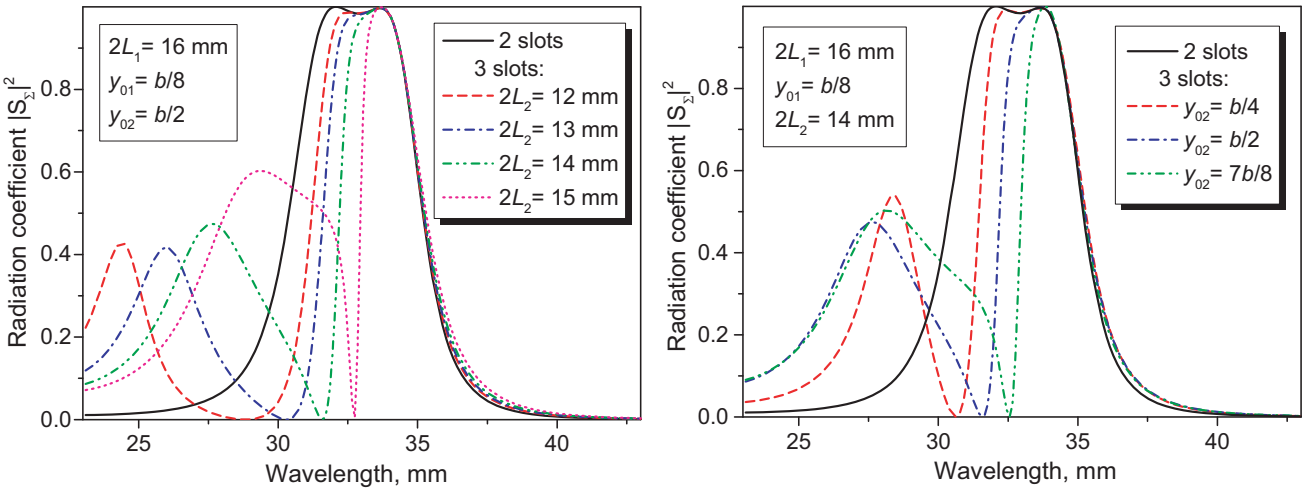

Figure 3. The power radiation coefficient versus the wavelength for the WSSA with one and two slot reentrant cavity.

where λ_c is a critical wavelength of the H_{10}-wave, and $\alpha = 1/\{8\ln[d_2/(8L_2)]\}$ is the small parameter,

$$
\begin{aligned}
F\left(a,b,L_2,d_{e2},y_{02}\right) \cong\ & 2\pi\left\{\frac{4\cos^2\dfrac{\pi L_2}{a}}{\gamma_{10}^2 a L_2}\left[\begin{array}{l}\dfrac{2\pi\cos^2\dfrac{\pi y_{02}}{b}}{k_{11}b}-2\cos^2\dfrac{\pi y_{02}}{b}\\ +\left(\dfrac{\gamma_{10}b}{9}\right)^2\cos^2\dfrac{2\pi y_{02}}{b}-\ln\left(\dfrac{\pi d_{e2}}{2b}\sin\dfrac{\pi y_{02}}{b}\right)\end{array}\right]\right.\\
&-\frac{4\cos^2\dfrac{3\pi L_2}{a}}{k_{30}^2 a L_2}\left[K_0\left(k_{30}\frac{d_{e2}}{4}\right)+K_0(2k_{30}y_{02})\right]+\left(\ln\frac{16L_2}{d_{e2}}-1\right)\\
&-\ln\frac{1-L_2/a}{1+L_2/a}+\ln\frac{1-2L_2/a}{1+2L_2/a}+\ln\frac{1-2L_2/(3a)}{1+2L_2/(3a)}\\
&\left.-\frac{a}{2L_2}\left[\ln\left(1-\left(\frac{2L_2}{a}\right)^2\right)-2\ln\left(1-\left(\frac{L_2}{a}\right)^2\right)+3\ln\left(1-\left(\frac{2L_2}{3a}\right)^2\right)-\left(\frac{L_2}{a}\right)^2\right]\right.
\end{aligned}
$$

$$-\frac{4a}{\pi^2 L_2}\left[K_0\left(\frac{\pi d_{e2}}{4a}\right)\sin^2\frac{\pi L_2}{a}+\frac{1}{9}K_0\left(\frac{3\pi d_{e2}}{4a}\right)\sin^2\frac{3\pi L_2}{a}+\sum_{m=5,7\ldots}^{\infty}K_0\left(\frac{m\pi d_{e2}}{4a}\right)/m^2\right]\Bigg\}. \quad (16)$$

Here $\gamma_{10}=\sqrt{(\pi/(2L_2))^2-(\pi/a)^2}$, $k_{11}=\sqrt{(\pi/a)^2+(\pi/b)^2-(\pi/(2L_2))^2}$, $k_{30}=\sqrt{(3\pi/a)^2-(\pi/(2L_2))^2}$, $K_0(x)$ is Macdonald function. Since the function $K_0(x)$ decreases rapidly with increasing argument, only the first few terms should be taken into account in the series of Eq. (16).

By varying the length H of the reentrant cavity, maximum radiation can be achieved at one or several wavelengths (Fig. 4: $2L_2 = 14.0\,\text{mm}$, $y_{02} = 7b/8$), while the value λ_{res}/λ_c is practically independent of the reentrant cavity dimensions.

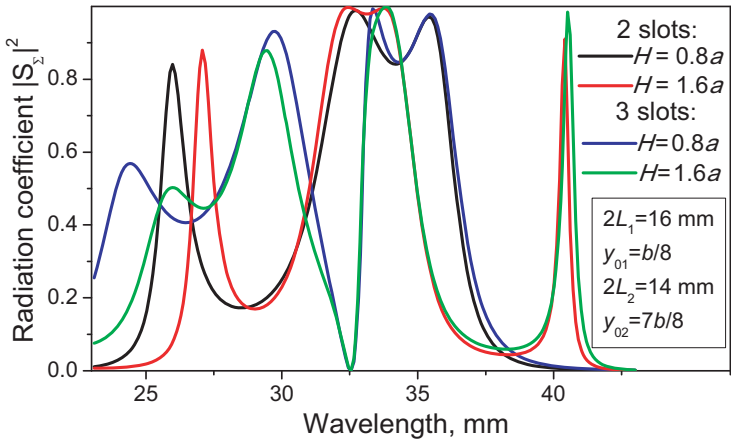

Figure 4. The WSSA power radiation coefficient versus the wavelength for various length H of the reentrant cavity.

The typical normalized RPs of the WSSA shown in Fig. 1, *c* are shown in Fig. 5. The plots were obtained with the following parameters: $\lambda = 32\,\text{mm}$, $R = \lambda\,\text{mm}$, $2L_3^e = 0.5\lambda$, and $d_3 = 0.05\lambda$. Note that in *E*-plane RP of the slot radiator placed over the infinite flat screen is presented by the constant function, while the *E*-plane RP of WSSA is significantly non-constant. The degree of the difference between the two cases increases when the sphere radius is decreased.

The validity of the numerical simulation was confirmed by comparing the calculated and experimental data. A photograph of a prototype WSSA model used for experimental studies is shown

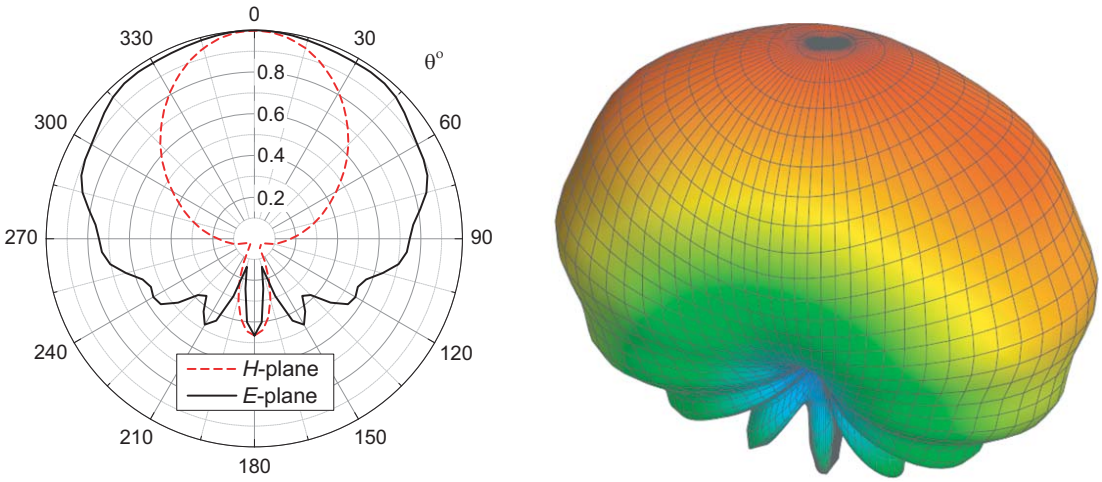

Figure 5. The RPs of the WSSA.

Figure 6. The prototype WSSA model.

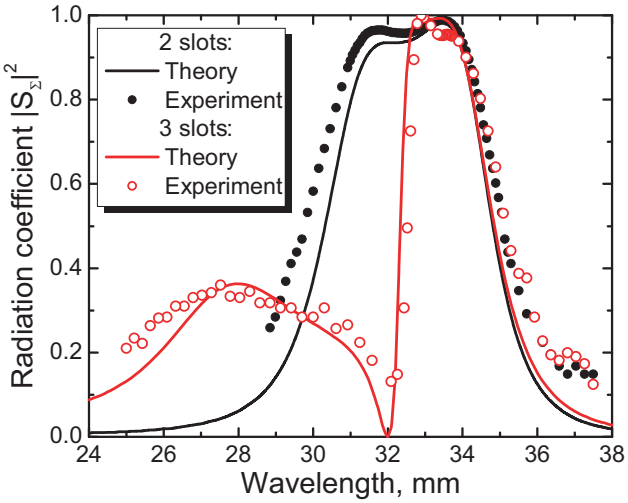

Figure 7. The power radiation coefficient of the WSSA versus the wavelength: $R = 50\,\text{mm}$, $a = 23\,\text{mm}$, $b = 10\,\text{mm}$, $2L_3^e = 18\,\text{mm}$, $d_m = 1.5\,\text{mm}$, $h_m = 2.0\,\text{mm}$, $2L_1 = 16.0\,\text{mm}$, $2L_2 = 14.0\,\text{mm}$, $H = a/2$, $y_{01} = y_{03} = b/4$, $y_{02} = 3b/4$.

in Fig. 6. The WSSA geometrical parameters and waveguide wall thickness for the standard rectangular waveguide are given in the caption of Fig. 7. The plots show that the theoretical curves and experimental data are in good agreement with each other.

5. CONCLUSION

The problem concerning radiation of electromagnetic waves into space outside the perfectly conducting sphere through a narrow slot cut in the end wall of the semi-infinite rectangular waveguide with the reentrant cavity in it is solved by the generalized method of induced MMF. The problem was solved by using the basis functions obtained as the analytical solutions of the integral equations for the slot currents by the asymptotic averaging method. The concept of equivalent slot width was introduce allowing us to eliminate the need to determine the fields in the internal slot cavities. The proposed mathematical model was verified by comparing the numerical results and experimental data. The results can be used in the design and development of WSSAs.

APPENDIX A. MAGNETIC GREEN'S FUNCTIONS OF THE CONSIDERED ELECTRODYNAMIC VOLUMES

1. The hollow half-infinite rectangular waveguide of the cross-section $\{a \times b\}$ with the perfectly conducting walls:

$$\begin{aligned}\hat{G}^m(\vec{r},\vec{r}') = \frac{2\pi}{ab}\sum_{m,n}\frac{\varepsilon_m\varepsilon_n}{k_z}\Big\{&(\vec{e}_x\otimes\vec{e}_x')\Phi_x^m(x,y;x',y')\left[e^{-k_z|z-z'|}+e^{-k_z(z+z')}\right]\\ &+(\vec{e}_y\otimes\vec{e}_y')\Phi_y^m(x,y;x',y')\left[e^{-k_z|z-z'|}+e^{-k_z(z+z')}\right]\\ &+(\vec{e}_z\otimes\vec{e}_z')\Phi_z^m(x,y;x',y')\left[e^{-k_z|z-z'|}-e^{-k_z(z+z')}\right]\Big\}.\end{aligned} \tag{A1}$$

The following symbols are accepted in Eq. (A1):

$$\begin{aligned}\Phi_x(x,y;x',y') &= \cos k_x x\cos k_x x'\sin k_y y\sin k_y y',\\ \Phi_y(x,y;x',y') &= \sin k_x x\sin k_x x'\cos k_y y\cos k_y y',\\ \Phi_z(x,y;x',y') &= \sin k_x x\sin k_x x'\sin k_y y\sin k_y y',\end{aligned}$$

$\varepsilon_{m,n}=\begin{cases}1, & m,n=0\\ 2, & m,n\neq 0\end{cases}$, $Rk_x=\frac{m\pi}{a}$, $k_y=\frac{n\pi}{b}$, $k_z=\sqrt{k_x^2+k_y^2-k^2}$, m and n are the integral numbers; $\vec{e}_x$, $\vec{e}_y$ and $\vec{e}_z$ are the unit vectors of the rectangular coordinate system; $\hat{I}=(\vec{e}_x\otimes\vec{e}_x')+(\vec{e}_y\otimes\vec{e}_y')+(\vec{e}_z\otimes\vec{e}_z')$ is the unit dyadic, and "$\otimes$" stands for dyadic product.

2. The hollow rectangular resonator $\{a_R\times b_R\times H\}$ with perfectly conducting walls:

$$\begin{aligned}\hat{G}^m(\vec{r},\vec{r}') &= \frac{2\pi}{a_R b_R}\sum_{m=0}^{\infty}\sum_{n=0}^{\infty}\frac{\varepsilon_m\varepsilon_n}{k_z}\\ &\times\Bigg\{(\vec{e}_x\otimes\vec{e}_x')\Phi_x^m(x,y;x',y')\left[\frac{chk_z(H-|z-z'|)+chk_z(H-|z+z'|)}{shk_zH}\right]\\ &+(\vec{e}_y\otimes\vec{e}_y')\Phi_y^m(x,y;x',y')\left[\frac{chk_z(H-|z-z'|)+chk_z(H-|z+z'|)}{shk_zH}\right]\\ &+(\vec{e}_z\otimes\vec{e}_z')\Phi_z^m(x,y;x',y')\left[\frac{chk_z(H-|z-z'|)-chk_z(H-|z+z'|)}{shk_zH}\right]\Bigg\}.\end{aligned} \tag{A2}$$

The following notations are adopted in Eq. (A2):

$$\begin{aligned}\Phi_x^m(x,y;x',y') &= \sin k_x x\sin k_x x'\cos k_y y\cos k_y y',\\ \Phi_y^m(x,y;x',y') &= \cos k_x x\cos k_x x'\sin k_y y\sin k_y y',\\ \Phi_z^m(x,y;x',y') &= \cos k_x x\cos k_x x'\cos k_y y\cos k_y y'.\end{aligned}$$

The remaining notations coinside with that in Eq. (A1).

3. Space outside the perfectly conducting sphere of the radius $\tilde{R}=R$ with the permittivity ε_1 and the permeability μ_1 of the medium (Fig. A.1):

$$\hat{G}^m\left(\rho,\theta,\varphi;\rho',\theta',\varphi'\right) = \begin{vmatrix} G^m_{\rho\rho'} & 0 & 0\\ 0 & G^m_{\theta\theta'} & G^m_{\theta\varphi'}\\ 0 & G^m_{\varphi\theta'} & G^m_{\varphi\varphi'}\end{vmatrix}, \tag{A3}$$

$$G^m_{\rho\rho'}\left(\rho,\theta,\varphi;\rho',\theta',\varphi'\right) = -\sum_{n=0}^{\infty}\sum_{m=0}^{n}\frac{\varepsilon_m\, h_n^m(\rho,\rho')}{2C_{nm}}P_n^m(\cos\theta)P_n^m\left(\cos\theta'\right)\cos m(\varphi-\varphi'),$$

$$G^m_{\theta\theta'}\left(\rho,\theta,\varphi;\rho',\theta',\varphi'\right) = -\sum_{n=0}^{\infty}\sum_{m=0}^{n}\frac{\varepsilon_m u_n^m(\rho,\rho')\cos m(\varphi-\varphi')}{2n\,(n+1)\,C_{nm}\sin\theta\sin\theta'}$$

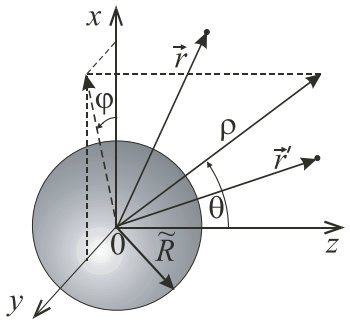

Figure A1.

$$\times \left[m^2 P_n^m(\cos\theta) P_n^m(\cos\theta') + \sin\theta \sin\theta' \frac{dP_n^m(\cos\theta)}{d\theta} \frac{dP_n^m(\cos\theta')}{d\theta'} \right],$$

$$G^m_{\theta\varphi'}(\rho,\theta,\varphi;\rho',\theta',\varphi') = \sum_{n=0}^{\infty}\sum_{m=0}^{n} \frac{m u_n^m(\rho,\rho') \sin m(\varphi-\varphi')}{n(n+1) C_{nm}} \times \left[\frac{dP_n^m(\cos\theta)}{d\theta} \frac{P_n^m(\cos\theta')}{\sin\theta'} + \frac{P_n^m(\cos\theta)}{\sin\theta} \frac{dP_n^m(\cos\theta')}{d\theta'} \right],$$

$$G^m_{\varphi\theta'}(\rho,\theta,\varphi;\rho',\theta',\varphi') = -G^m_{\theta\varphi'}(\rho,\theta,\varphi;\rho',\theta',\varphi'),$$

$$G^m_{\varphi\varphi'}(\rho,\theta,\varphi;\rho',\theta',\varphi') = G^m_{\theta\theta'}(\rho,\theta,\varphi;\rho',\theta',\varphi').$$

Here $P_n^m(\cos\theta)$ is the associated Legendre functions of the first sort,

$$C_{nm} = \frac{2\pi(n+m)!}{(2n+1)(n-m)!},$$

$$h_n^m(\rho,\rho') = \begin{cases} 4\pi k_1 h_n^{(2)}(k_1\rho') \begin{bmatrix} j_n(k_1\rho) Q_n\left(y_n\left(k_1\tilde{R}\right)\right) \\ -y_n(k_1\rho) Q_n\left(j_n\left(k_1\tilde{R}\right)\right) \end{bmatrix}, & \tilde{R} \le \rho < \rho', \\ 4\pi k_1 h_n^{(2)}(k_1\rho) \begin{bmatrix} j_n(k_1\rho') Q_n\left(y_n\left(k_1\tilde{R}\right)\right) \\ -y_n(k_1\rho') Q_n\left(j_n\left(k_1\tilde{R}\right)\right) \end{bmatrix}, & \rho > \rho', \end{cases},$$

$$Q_n(f_n(k_1R)) = \frac{n f_n\left(k_1\tilde{R}\right) - k_1\tilde{R} f_{n+1}\left(k_1\tilde{R}\right)}{n h_n^{(2)}\left(k_1\tilde{R}\right) - k_1\tilde{R} h_{n+1}^{(2)}\left(k_1\tilde{R}\right)},$$

$$u_n^m(\rho,\rho') = \begin{cases} 4\pi k_1 \dfrac{h_n^{(2)}(k_1\rho')}{h_n^{(2)}\left(k_1\tilde{R}\right)} \left[j_n(k_1\rho) y_n\left(k_1\tilde{R}\right) - y_n(k_1\rho) j_n\left(k_1\tilde{R}\right) \right], & \tilde{R} \le \rho < \rho', \\ 4\pi k_1 \dfrac{h_n^{(2)}(k_1\rho)}{h_n^{(2)}\left(k_1\tilde{R}\right)} \left[j_n(k_1\rho') y_n\left(k_1\tilde{R}\right) - y_n(k_1\rho') j_n\left(k_1\tilde{R}\right) \right], & \rho > \rho', \end{cases}$$

$h_n^{(2)}(k_1\rho) = j_n(k_1\rho) - iy_n(k_1\rho) = \sqrt{\frac{\pi}{2k_1\rho}} H^{(2)}_{n+1/2}(k_1\rho)$ is the Hankel spherical function of the second sort; $j_n(k_1\rho) = \sqrt{\frac{\pi}{2k_1\rho}} J_{n+1/2}(k_1\rho)$ and $y_n(k_1\rho) = \sqrt{\frac{\pi}{2k_1\rho}} N_{n+1/2}(k_1\rho)$ are the Bessel spherical function and the Neumann one, correspondingly; $J_{n+1/2}(k_1\rho)$ is the Bessel function; $N_{n+1/2}(k_1\rho)$ is the Neumann function, and $H^{(2)}_{n+1/2}(k_1\rho)$ is the Hankel function of the second sort with the half-integral index.

REFERENCES

1. Lewin, L., *Advanced Theory of Waveguides*, Iliffe & Sons, London, 1951.
2. Mittra, R., *Computer Techniques for Electromagnetics*, Pergamon Press, NY, 1973.
3. Reznikov, G. B., *Antennas of Flying Vehicles*, Soviet Radio, Moscow, 1967 (in Russian).
4. Schantz, H., "Nanoantennas: A concept for efficient electrically small UWB devices," *IEEE International Conference ICU 2005*, 264–268, Sept. 2005.
5. Vorst, A. V., A. Rosen, and Yu. Kotsuka, *RF/Microwave Interaction with Biological Tissues*, Willey-IEEE Press, NY, 2006.
6. Mushiake, Y. and R. E. Webster, "Radiation characteristics with power gain for slots on a sphere," *IRE Trans. Antennas Propagat.*, Vol. 5, 47–55, 1957.
7. Leung, K. W., "Theory and experiment of a rectangular slot on a sphere," *IEEE Trans. Microwave Theory Tech.*, Vol. 46, 2117–2123, 1998.
8. Kwok, W. L., "Rectangular and zonal slots on a sphere with a backing shell: Theory and experiment," *IEEE Trans. Antennas Propagat.*, Vol. 51, 1434–1442, 2003.
9. Berdnik, S. L., Yu. M. Penkin, V. A. Katrich, M. V. Nesterenko, and V. I. Kijko, "Electromagnetic waves radiation into the space over a sphere by a slot in the end-wall of a semi-infinite rectangular waveguide," *Progress In Electromagnetics Research B*, Vol. 46, 139–158, 2013.
10. Berdnik, S. L., V. A. Katrich, M. V. Nesterenko, and Yu. M. Penkin, "Spherical antenna excited by a slot in an impedance end-wall of a rectangular waveguide," *Proc. of the XVIII-th International Seminar/Workshop on Direct and Inverse Problems of Electromagnetic and Acoustic Wave Theory*, 111–114, Lviv, Ukraine, 2013.
11. Berdnik, S. L., V. A. Katrich, Yu. M. Penkin, M. V. Nesterenko, and S. V. Pshenichnaya, "Energy characteristics of a slot cut in an impedance end-wall of a rectangular and radiating into the space over a perfectly conducting sphere," *Progress In Electromagnetics Research M*, Vol. 34, 89–97, 2014.
12. Berdnik, S. L., V. S. Vasylkovskyi, M. V. Nesterenko, and Yu. M. Penkin, "Radiation fields of the spherical slot antenna in a material medium," *Proc. of the X-th Anniversary International Conference on Antenna Theory and Techniques*, Kharkiv, Ukraine, 282–284, 2015.
13. Nesterenko, M. V., V. A. Katrich, Yu. M. Penkin, and S. L. Berdnik, *Analytical and Hybrid Methods in Theory of Slot-Hole Coupling of Electrodynamic Volumes*, Springer Science+Business Media, New York, 2008.
14. Long, S. A., "Experimental study of the impedance of cavity-backed slot antennas," *IEEE Trans. Antennas Propag.*, Vol. 23, 1–7, 1975.
15. Lee, J. Y., T. Sh. Horng, and N. G. Alexopoulos, "Analysis of cavity-backed aperture antennas with a dielectric overlay," *IEEE Trans. Antennas Propag.*, Vol. 42, 1556–1562, 1994.
16. Nesterenko, M. V. and V. A. Katrich, "The method of induced magnetomotive forces for cavity-backed slot radiators and coupling slots," *Radioelectronics and Communications Systems*, Vol. 47, 8–13, 2004.
17. Mittra, R. and S. W. Lee, *Analytical Techniques in the Theory of Guided Waves*, Collier-Macmillan Limited, London, 1971.